

# Regulation of *in vivo* behaviour of TAT-modified liposome by associated protein corona and avidity to tumor cells

Mohamadreza Amin<sup>1,2,3</sup>

Mahsa Bagheri<sup>3</sup>

Mercedeh Mansourian<sup>3</sup>

Mahmoud Reza Jaafari<sup>3\*</sup>

Timo L.M. ten Hagen<sup>1\*</sup>

<sup>1</sup>Laboratory Experimental Surgical Oncology, Section Surgical Oncology, Department of Surgery, Erasmus Medical Center, Rotterdam, The Netherlands

<sup>2</sup> Cellular and Molecular Research Center, Faculty of Medicine, Sabzevar University of Medical Sciences, Sabzevar, Iran

<sup>3</sup> Biotechnology Research Center, Pharmaceutical Technology Institute, Mashhad University of Medical Sciences, Mashhad, Iran

\*Correspondence:

Timo L.M. ten Hagen

P.O. Box 2040, 3000 CA Rotterdam, The Netherlands

Tel : +31107043682

Fax : +31107044746 Email : t.l.m.tenhagen@erasmusmc.nl

Mahmoud R. Jaafari

P.O. Box: 91775-1365, Mashhad, Iran

Tel: +98 51 31801336

Fax: +98 51 38823251

E-mail: jafarimr@mums.ac.ir

## Supplementary data:

### ***Conjugation of TAT to DSPE-PEG2000-Maleimide***

TAT peptide was dissolved in DMSO in concentration of 10 mg/mL and added to chloroform solution of DSPE-PEG2000-Maleimide. The volumes were adjusted to reach chloroform:DMSO ratio of 50:50 (v/v) with molar ratio of 1.1 peptide to 1 lipid. The mixture was then incubated overnight at room temperature with gentle stirring. Samples of free TAT peptide, free DSPE-PEG2000-Mal, and a sample of conjugation mixture were withdrawn and analyzed by MALDI-TOF to confirm the conjugation. As illustrated in Figure 1, the corresponding mass spectral (MALDI-TOF) data for the free TAT peptide, free DSPE-PEG2000-Mal (Figure 1A and B), and a sample of conjugation mixture revealed the consumption of free DSPE-PEG2000-Mal in reaction (Figure 1C) and formation of the DSPE-PEG-TAT lipopeptide (Figure 1D). Finally the mixture was assayed for phospholipid content and aliquots of conjugated mixture with defined amount of lipopeptide (quantified by phosphorus assay) were dried by nitrogen gas blowing followed by freeze drying and stored at -70°C.

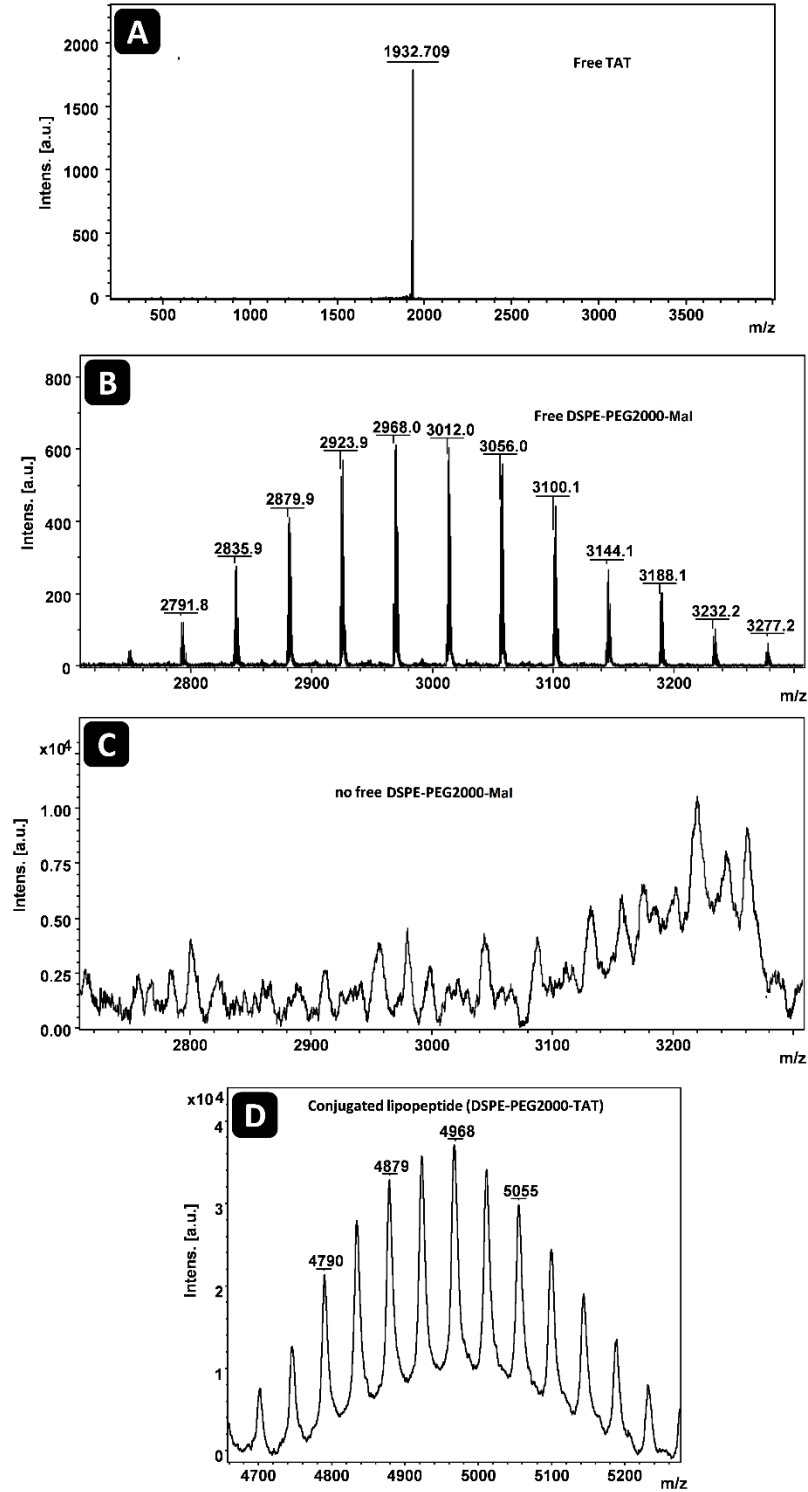


**Figure 1** The corresponding mass spectral (MALDI-TOF) data for (A): free TAT peptide, (B): DSPE-PEG2000-Mal, (C): consumption of the DSPE-PEG2000-Mal in reaction mixture as a result of conjugation and formation of the (D) DSPE-PEG-TAT lipopeptide conjugate.

## ***Preparation of DiO-labeled PLD-TAT***

Fluorescent labeled liposomes (PLF) composed of HSPC, mPEG2000-DSPE, cholesterol,  $\alpha$ -tocopherol and the lipophilic dye (56.1:5.5:38.2:0.1:0.1) was prepared by solvent evaporation plus sonication and extrusion and doxorubicin (DXR) was remotely loaded into liposomes using ammonium gradient method. Briefly, Lipids were dissolved in chloroform and dried by rotary evaporator and overnight connection to freeze drier, hydrated in ammonium sulfate 250 mM and downsized by 10 min bath sonication and extrusion through polycarbonate membranes of 200 nm and 80 nm sequentially, using LIPEX<sup>TM</sup> (Northern lipid Inc. Vancouver, Canada). Ammonium sulfate liposomes were then dialyzed against sucrose 10% using Nessler's reagent to confirm buffer exchange and formation of ammonium gradient. Doxorubicin was then added into liposomes (1 mg doxorubicin per 10  $\mu$ mol of total lipid) and incubated for 1 h at 65 °C, cooled to room temperature, mixed with Dowex<sup>®</sup> resin (60 mg Dowex<sup>®</sup> per 1 mg doxorubicin) and rotated for 60 min in order to remove free doxorubicin and finally run through Poly-Prep columns (Bio-Rad Laboratories Inc.) to remove Dowex<sup>®</sup>. Liposomal suspension was then sterilized by passing through syringe filter (0.2  $\mu$ ) and assayed for phospholipid content. From that the required amount of TAT-lipopeptide to create the desired surface density of TAT on liposome was calculated and post inserted into liposomes as described in the main article.

## ***Leakage stability assessments of PLD-TATs***

Leakage stability of TAT modified PLDs and non-modified PLD (Caelyx<sup>®</sup>) was evaluated during postinsertion of DSPE-PEG-TAT and also during incubation at 37°C in the presence of 30% FCS. Samples were withdrawn from PLDs before and after postinsertion or at different time points after incubation with 30% FCS at 37°C. Samples were then centrifuged on centrifugal filter device (Amicon Ultra-0.5 mL Centrifugal Filters MWCO: 3000) for 5 min at 6000 g and the concentration of free DXR passed through the filter was assayed. Percent of DXR remained encapsulated was then calculated. Data represent as mean  $\pm$  SD (n = 4).

## ***Cell culturing***

C26 colon carcinoma cells and B16F0 melanoma cells were cultured at 37 °C in a 5% CO<sub>2</sub> /95% air humidified atmosphere in RPMI1640 and DMEM mediums, respectively.. Mediums contained 25 mM HEPES and 2 mM L-glutamine and were supplemented with 10% (v/v) heat-inactivated FCS, 100 IU/ml penicillin and 100 mg/ml streptomycin.

## Colloidal properties of TAT-modified liposomes

Liposomes were characterized with respect to size, polydispersity index and  $\zeta$ -potential by a Dynamic Light Scattering instrument (Nano-ZS; Malvern, UK) at 25 °C with a scattering angle of 173° (Table 1). As soon as micellar DSPE-PEG-TAT was added to liposomes, the transparent liposomal suspension became turbid, presumably due to formation of electrostatic cross-bridges between a positively charged micelle and few negatively charged liposomes forming a larger particle that changes the optical properties of the nanoliposomal dispersion. However, within around 5 minutes of incubation at 50 °C we observed that the solution returned to the initial transparent (opaque) state. Since micelles that are in contact with liposomal bilayer are unstable at elevated temperatures [39], it is likely that through transfer of micellar lipopeptides into liposomal bilayer, the positive core and consequently the cross bridges disappeared and the liposomal suspension shows nano-optical properties while showing a narrow PDI.

**Table 1** Colloidal properties of fluorescently-labeled PEGylated liposomes (FPLs) and PEGylated liposomes containing doxorubicin (PLDs)

Preparation name	Density of surface inserted TAT (Peptides/ liposome)	$\zeta$ -Average (nm)	PDI	$\zeta$ Potential (mv)
DiO-FPL-Plain	0	101±2.6	0.065	-25.6 ± 4.3
DiO-FPL-TAT25	25	103±3.2	0.052	-23.7 ±7.5
DiO-FPL-TAT50	50	100±2.7	0.031	-25.7 ± 6.5
DiO-FPL-TAT100	100	99±3.3	0.022	-22.1 ± 5.3
DiO-FPL-TAT200	200	102±4.2	0.078	-23.4 ± 4
DiO-FPL-TAT300	300	100±3.2	0.035	-19 ± 3.7
DiO-FPL-TAT400	400	101±5.1	0.081	-17 ± 4.7
Caelyx®	0	93.7 ± 3.2	0.021	-25.3 ± 3.8
PLD-TAT25	25	94.2 ± 3.1	0.014	-24.2± 4.5
PLD-TAT50	50	95.7 ± 2.9	0.032	-23.3 ± 5.4
PLD-TAT100	100	93.6 ± 4.3	0.051	-23.4 ± 4.7
PLD-TAT200	200	94.1 ± 5.2	0.065	-22.1 ± 5.6
DiD-FPL-TAT200	200	109 ± 8.1	0.091	-21.43 ± 3.9

Data represented as mean ± SD of three (n=3) different measurements carried out for each sample in HEPE 10 mM, NaCl 135 mM, pH

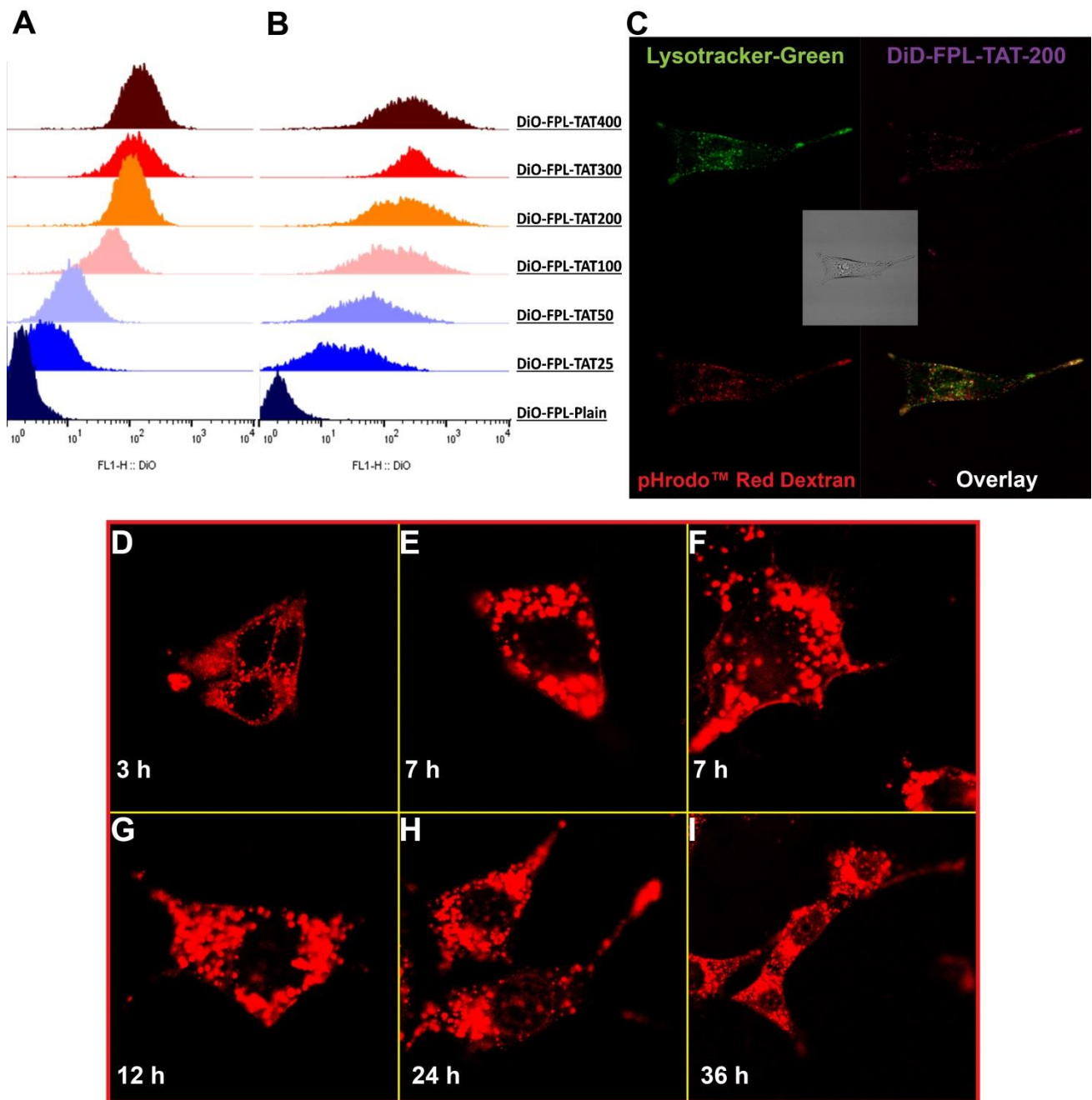


**Figure 2** Histograms of FACS analysis of cellular association FPLs with cells including B16 (A), C-26 (B). Cells ( $10^5$  cell/well) were exposed to 100 nmol liposomal phospholipid/500  $\mu$ l for 3 h at 37 °C, detached and association of liposomes with cells was analyzed by flowcytometry. Panel C illustrates the co-localization of internalized DiD-FPL-TAT-200 with both endocytosis marker pHrodo™ Red Dextran and lysosomal marker Lysotracker-Green after 3 h of exposure of lysosomal pre-stained B16 cells with liposomes and pHrodo™ Red Dextran (20  $\mu$ g/m). Images D-I illustrate the intracellular fate of DXR internalized into C-26 cells after 3 h of exposure of cells with PLD-TAT200 followed by washing. Images captured at different time points after liposome-cell exposure.

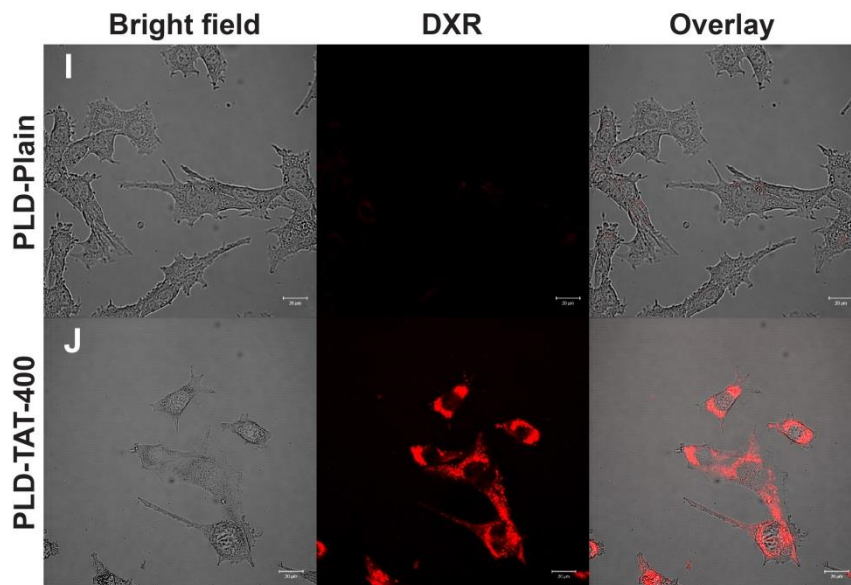
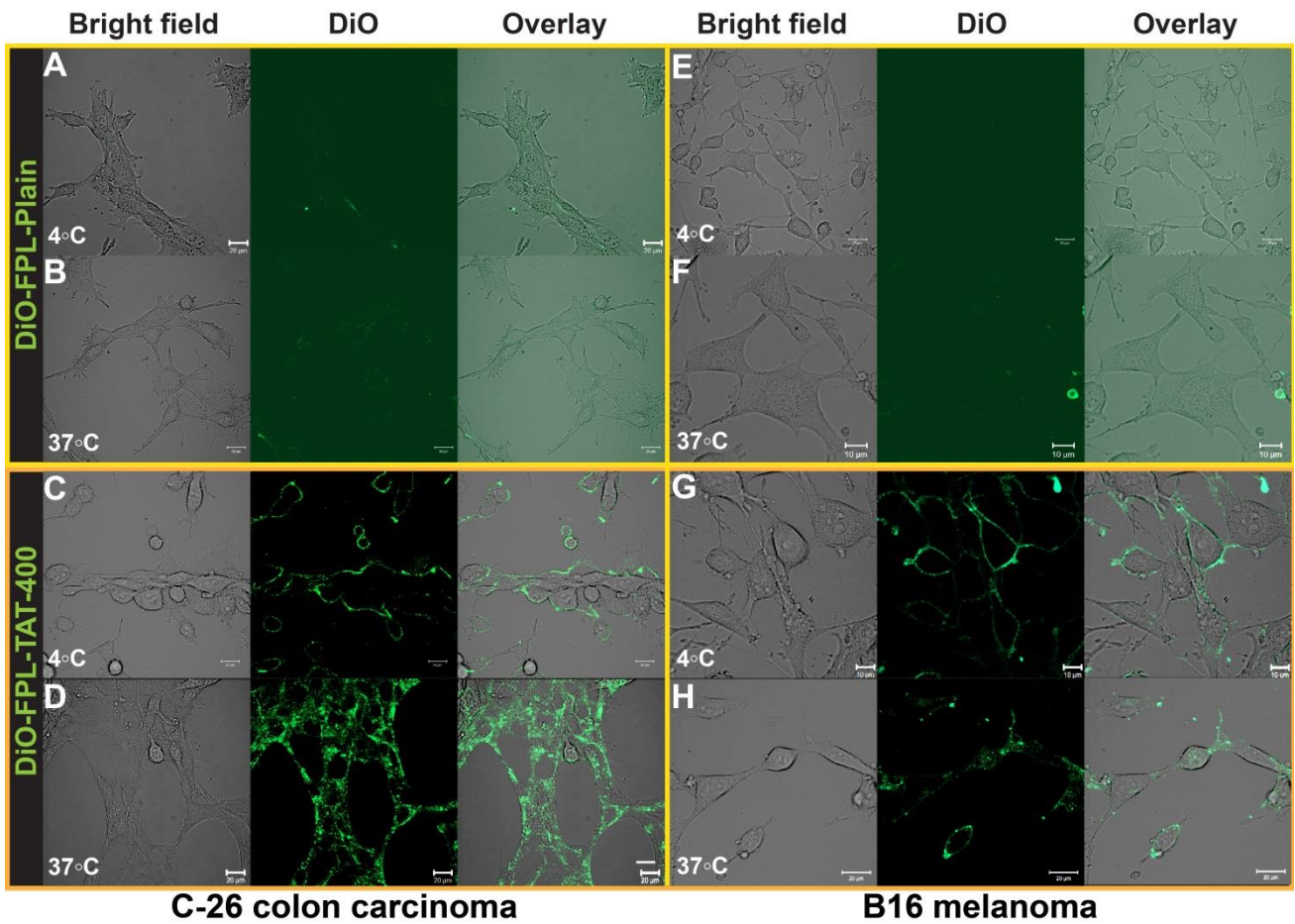


**Figure 3** Cellular association of TAT-modified and Plain liposomes. (A-H) illustrate the association of DiO labeled TAT-modified liposomes or non-modified (Plain) liposomes with C-26 colon carcinoma or B16 murine melanoma cells at either 4°C or 37°C. Panels I and J, respectively, illustrate association of PLD-Plain and

PLD-TAT-400 with C-26 cells at 37 °C. Cells ( $10^5$ ) were exposed to 50 nmol liposomal phospholipid/500  $\mu$ Lit for 3h, washed and imaged.

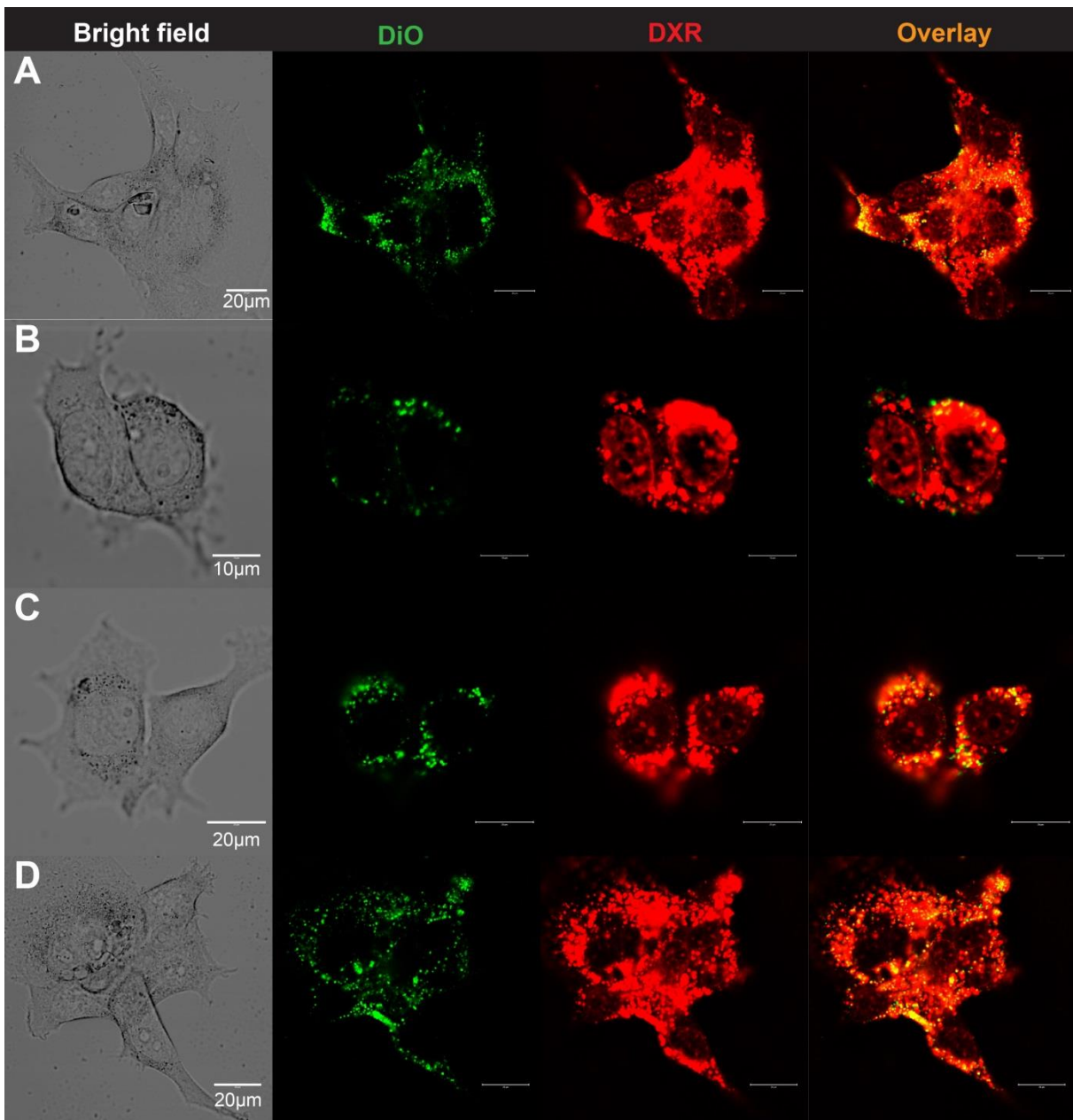


**Figure 4** Images of intracellular fate of DXR delivered to C-26 cells at 37 °C by PLD-TAT-400. Cells ( $10^5$ ) were exposed to 50 nmol liposomal phospholipid/500  $\mu$ Lit for 3h, washed and imaged after 24 h.



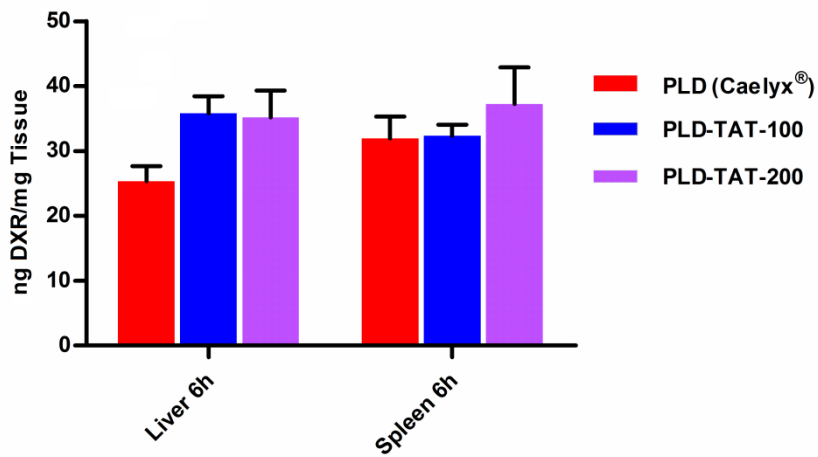


**Figure 5:** Doxorubicin concentration (ng/mg tissue) in liver and spleen of mice at 6 h after a single i.v injection of 15 mg/kg DXR encapsulated in different PLD-TATs. Data represent mean  $\pm$  SE (n=3).

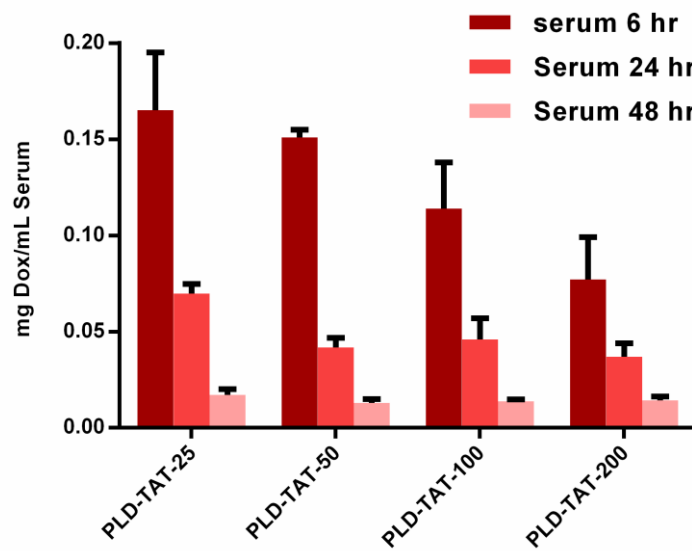


**Figure 6** Concentration of DXR at different time points in serum of BALB/c mice bearing C-26 tumor after a single i.v injection of 15 mg/kg liposomal DXR. Serums were separated by high centrifugation of 14000 g  $\times$  10 min. Data represent mean  $\pm$  SD (n=4).

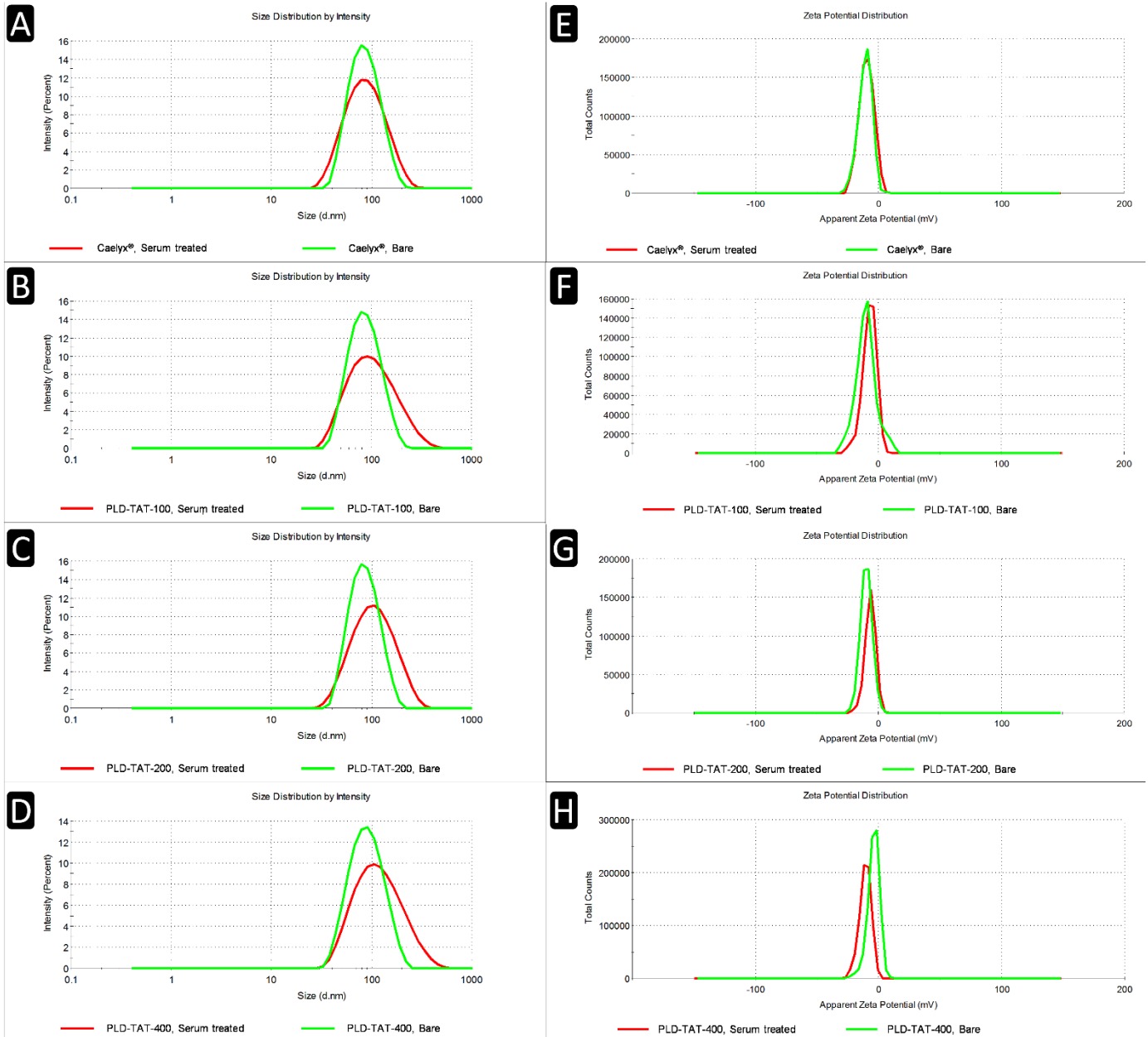


**Figure 7** Effect of protein corona formation on colloidal properties of liposomes. Panels A-D illustrate the size distribution by intensity and panels E-F illustrate the zeta potential distribution of liposomes including Caelyx<sup>®</sup> (A and E), PLD-TAT-100 (B and F), PLD-TAT-200 (C and G) and PLD-TAT-400 (D and H) before (green line) and after (red line) incubation with mice serum.

**Table 2** colloidal properties of PLDs before and after serum treatment

preparations	Non serum treated			Serum treated		
	Size ζ –Average (nm)	Pdi	ζ Potential (mv)	Size	Pdi	ζ Potential (mv)
Caelyx <sup>®</sup>	83.64 ± 3.04	0.17 ± 0.04	-9.94 ± 1.59	77.32 ± 0.18	0.26 ± 0.01	-10.03 ± 1.13
PLD-TAT-25	84.45 ± 2.91	0.19 ± 0.05	-9.31 ± 2.08	80.22 ± 0.39	0.31 ± 0.01	-9.58 ± 0.64
PLD-TAT-100	84.33 ± 3.41	0.18 ± 0.01	-7.31 ± 1.32	85.24 ± 0.44	0.28 ± 0.01	-9.91 ± 0.49
PLD-TAT-200	85.57 ± 2.84	0.12 ± 0.02	-6.80 ± 0.73	91.24 ± 0.28	0.27 ± 0.01	-9.92 ± 0.59
PLD-TAT-400	87.54 ± 2.20	0.15 ± 0.03	-4.43 ± 0.83	96.69 ± 0.89	0.33 ± 0.04	-9.63 ± 0.89

Data represented as mean ± SD of at least four (n=4) different measurements carried out for each sample in Tris-HCl 10 mM, NaCl 135 mM, pH 7.4.

### ***Effect of protein corona formation on liposome-cell interactions***

To investigate the effect of PC formation on *in vitro* association of FPL-TATs with tumor cells different studies were performed. First cells were exposed for 3 h to different FPL-TATs either as PC-free liposomes (without serum treatment) or PC-associated liposomes (with serum treatment). Results (Figure 8) indicated that PC formation did not completely inhibit liposomes cell association and even liposomes with low TAT density of 25 TAT/liposome were more active than non-modified liposomes. However, the highest inhibitory effect was found in non-modified FPL where association reduced by 80%. PC formation reduced the cell-association FPL-25 to FPL-400 by 59%, 32%, 30%, 21%, 17% and 27%, respectively. In fact protein corona could not inhibit liposome cell interaction but decreased the exposure rate of TAT moieties on outer surface of PEGylated liposomes, therefore preparations with lower TAT densities affected more.

However this brings a question whether TAT itself is responsible for the observed liposome-cell interaction or it is serum derived proteins that promote liposome cell interactions. To assess this TAT-FPL containing PC or without PC were exposed to cells in two different conditions. First it was found that in both PC-associated and bare liposomes, cell-association was blocked in same extent in presence of heparin which inhibits TAT interaction with proteoglycans of cell surface (Figure 9). In addition to this cells starved of serum did not showed enhanced uptake of PC-associated liposomes compared to cells cultured in normal condition (Figure 10). This reveals that even in serum-starved condition, similar to tumor interstitium where cells demand highly

to serum protein supply, PC-derived proteins on surface of liposomes cannot enhance liposome uptake by tumor cells, supporting the exclusive role of TAT-residues in induction of TAT-liposome uptake by tumor cells.

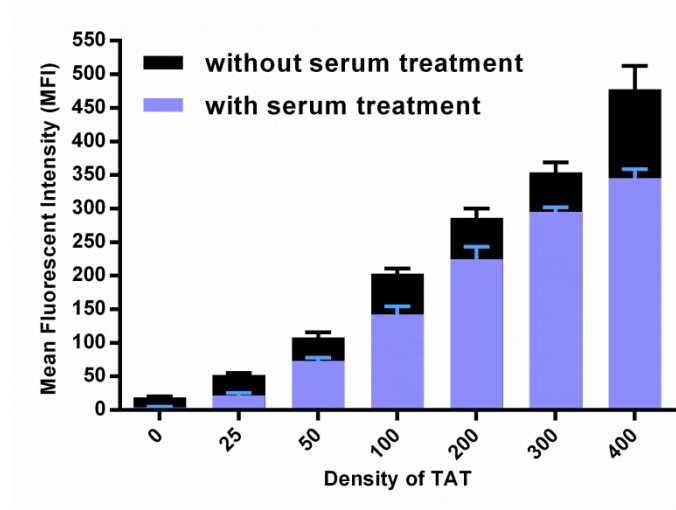


**Figure 8** Effect of protein corona formation on association of FPL-TATs with C-26 cells. Cells ( $10^5$  cell/well) were cultured overnight in complete culture medium and medium was replaced with 0.5 mL liposome containing medium (100 nmol liposomal phospholipid/500  $\mu$ L). liposomes without serum treatment were only diluted with FCS-free culture medium. For serum-treated liposomes, liposomes were first diluted with FCS (the volume required to make 10% FCS supplemented medium) and incubated at 37°C for 1 h and then added to FCS-free culture medium to make 100 nmol liposomal phospholipid/500  $\mu$ L plus 10% FCS. Cells were then exposed to liposomes for 3 h at 37 °C, detached and association of liposomes with cells was analyzed by flowcytometry.

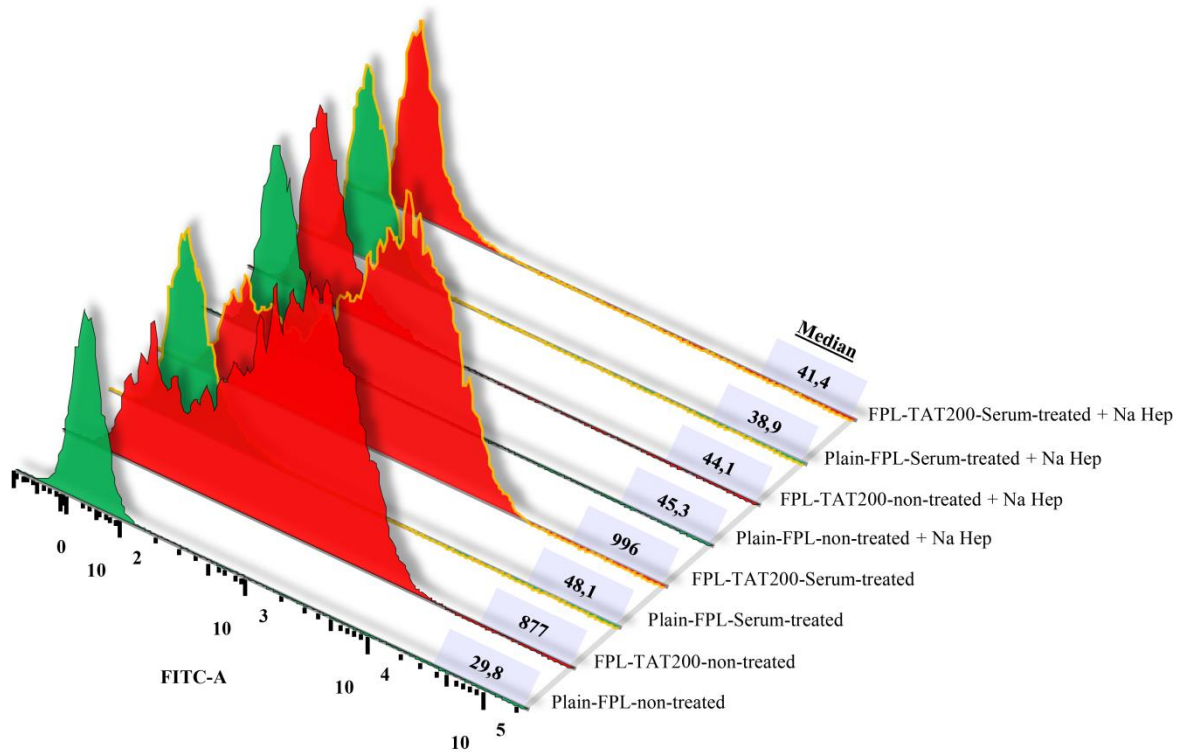


**Figure 9** Effect of sodium heparin (Na Hep) on association of C-26 cells with non-modified and TAT-modified FPLs either as non-treated or treated with serum. Cells ( $10^5$  cell/well) were first seeded and incubated overnight in complete culture medium and medium was replaced with 0.5 mL liposome containing medium (100 nmol liposomal phospholipid/500  $\mu$ L). liposomes without serum treatment were only diluted with FCS-free culture medium. For serum-treated liposomes, liposomes were first diluted with FCS (the volume required to make 10% FCS supplemented medium) and incubated at 37°C for 1 h and then added to FCS-free culture medium to make 100 nmol liposomal phospholipid/500  $\mu$ L plus 10% FCS. Na Hep (LEO Pharma, Ballerup, Denmark) was also added in concentration of 0.2 u.i./500  $\mu$ L in liposome containing suspension. Cells were then exposed to liposomes for 3 h at 37 °C, detached and association of liposomes with cells was analyzed by flowcytometry.

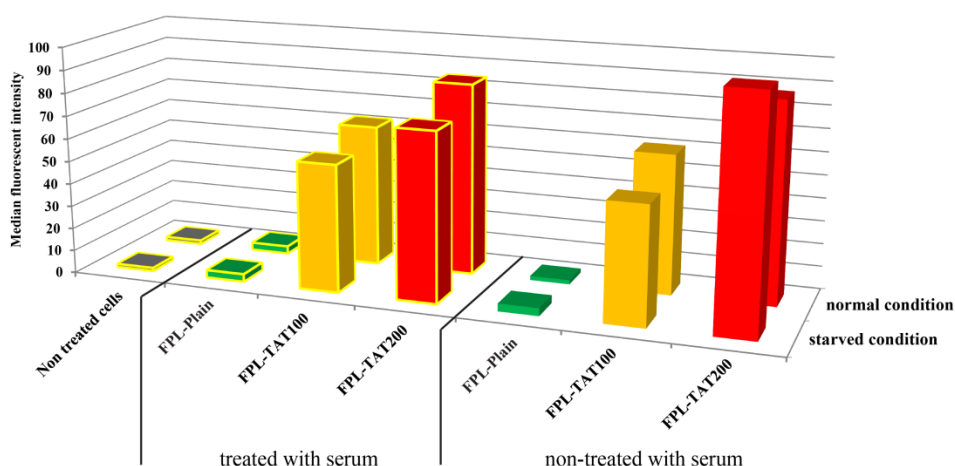


**Figure 10** Effect of protein corona formation on association of FPL-TATs with C-26 cells cultured in normal or starved condition. Normal Cells or cells starved of serum ( $10^5$  cell/well) were first cultured in complete or FCS-free culture medium, respectively. After overnight incubation medium was replaced with 0.5 mL liposome containing medium (100 nmol liposomal phospholipid/500  $\mu$ L). liposomes without serum treatment were only diluted with FCS-free culture medium. For serum-treated liposomes, liposomes were first diluted with FCS (the volume required to make 10% FCS supplemented medium) and incubated at 37°C for 1 h and then added to FCS-free culture medium to make 100 nmol liposomal phospholipid/500  $\mu$ L plus 10% FCS. Cells were then exposed to liposomes for 3 h at 37 °C, detached and association of liposomes with cells was analyzed by flowcytometry.

### ***Occurrence of skin necrosis in mice bearing C26 dermal tumor***

In compliance with the Institutional Ethical Committee and Research Advisory Committee of Mashhad University of Medical Sciences guidelines, female BALB/c mice were inoculated with a dermal injection of  $5 \times 10^5$  C26 colon carcinoma cells in the right flank. On day 10, when the tumor size was about 5 mm wide, mice with dermal tumors (5 per group) received a single dose of 15 mg/kg liposomal DXR via the tail vein. Tumor size and shape were then monitored daily. Manifestation of dry, thick, black eschar represents the occurrence of skin damage as a result of necrosis. Therefore, appearance of necrosis surrounding tumor, regardless of the degree of the skin damage (Figure 11), was used as a means of estimating the skin toxicity related to the treatments. Differences in the occurrence of dermal toxicity in dermal tumor mice were analyzed by contingency tables, using Fisher's exact test .

As tabulated in Table 3 from day 2 to 4 post injection mild (Figure 11 A and B) to more severe (Figure 11 C-F) necrotic lesions appeared in different treated group.

While Caelyx<sup>®</sup> caused no sign of necrosis, increasing the density of TAT increased the occurrence of necrosis at the tumor site. Of note is that no sign of tumor necrosis was seen in mice bearing s.c tumor in therapeutic efficacy studies indicating the dependency of necrosis occurrence to the tumor location.

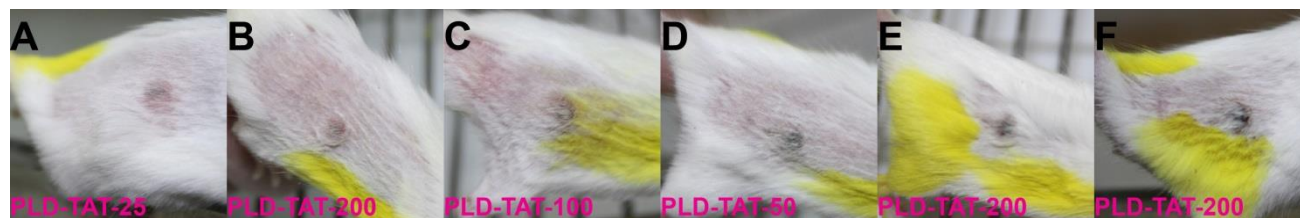


**Figure 11** Samples of mice with dermal tumors which showed necrosis of the skin followed by single iv injection of 15 mg/kg liposomal DXR encapsulated in different targeted on non-targeted liposomes.

**Table 3** Occurrence of necrosis corresponding to each treatment in BALB/C mice bearing dermal C-26 tumor after a single i.v injection of 15 mg/kg liposomal DXR

treatment	% of skin necrosis (No. BALB/c mice with necrosis/group)
Caelyx <sup>®</sup>	0
PLD-TAT-25 <sup>ns</sup>	33.3
PLD-TAT-50 <sup>ns</sup>	33.3
PLD-TAT-100 <sup>*</sup>	50
PLD-TAT-200 <sup>*</sup>	66.6

\*: statistically significant ( $p < 0.05$ ) compared to Caelyx<sup>®</sup>  
 ns: statistically non-significant ( $p > 0.05$ ) compared to Caelyx<sup>®</sup>